# Generation of pulse trains in nonlinear optical fibers through the generalized complex Ginzburg-Landau equation

Camus G. Latchio Tiofack,[1,*] Alidou Mohamadou,[2,3,†] Timoléon C. Kofané,[1,3,‡] and Alain B. Moubissi[4,§]
[1]*Laboratory of Mechanics, Department of Physics, Faculty of Science, University of Yaounde I, P.O. Box 812, Yaounde, Cameroon*
[2]*Condensed Matter Laboratory, Department of Physics, Faculty of Science, University of Douala, P.O. Box 24157, Douala, Cameroon*
[3]*The Max Planck Institute for the Physics of Complex Systems, Nöthnitzer Strasse 38, 01187 Dresden, Germany*
[4]*Département de Physique, Université des Sciences et Techniques de Masuku, BP 943, Franceville, Gabon*
(Received 4 March 2009; revised manuscript received 18 October 2009; published 10 December 2009)

We consider a higher-order complex Ginzburg-Landau equation, with the fourth-order dispersion and cubic-quintic nonlinear terms, which can describe the propagation of an ultrashort subpicosecond or femtosecond optical pulse in an optical fiber system. We investigate the modulational instability (MI) of continuous wave solution of this equation. Several types of modulational instability gains are shown to exist in both the anomalous and normal dispersion regimes. We find that depending on the sign of the fourth-order dispersion coefficient, the MI appears for normal and anomalous dispersion regime. Simulations of the full system demonstrate that the development of the MI leads to establishment of a regular or chaotic array of pulses, a chain of well-separated peaks with continuously growing or decaying amplitudes depending on the sign of the loss/gain coefficient and higher-order dispersions terms. Comparison of the calculations with reported numerical results shows a satisfactory agreement.

DOI: 10.1103/PhysRevE.80.066604 PACS number(s): 05.45.Yv, 42.65.Tg

## I. INTRODUCTION

Solitons are ubiquitous in nature, appearing in diverse systems such as shallow water waves, deoxyribonucleic acid-(DNA) excitations, matter waves in Bose-Einstein condensates, and ultrashort pulses (or laser beams) in nonlinear optics [1]. Originally, the terminology soliton was reserved for a particular set of integrable solutions existing as a result of the delicate balance between dispersion (or diffraction) and nonlinearity. The generation of a train of soliton pulses from continuous wave (CW) light in optical fibers was first suggested by Hasegawa and Tappert [2], and first realized experimentally by Mollenauer *et al.* [3]. Optical soliton are used for long and short-distance information transmission because, unlike pulses in a linear dispersive fiber, solitons are self-confined, propagating for a long distance without changing shape [3]. A well-known example of an equation which admits pulselike soliton solutions is the nonlinear Schrödinger (NLS) Eq. [4]. For long-distance communication systems, compensating for attenuation of pulses inherent in fibers is an important issue. One approach is the use of periodically spaced phase-sensitive amplifiers. Each of such amplifier exhibits an associated reference phase. The part of the signal in phase with this reference phase is amplified, while the out-of-phase component is attenuated [5]. In the second approach, the losses can be compensated by the erbium-doped amplified [6]. A well-known model for the study of pulse propagation in doped fiber amplifiers is the complex Ginzburg-Landau (CGL) Eq. [7]. The CGL equation of the simplest type has the cubic nonlinearity. In that case, exact solutions for pulses are available [8], but they are unstable. The most straightforward modification of the model, which opens the way to the existence of stable solitary pulses is the introduction of the cubic-quintic (CQ) nonlinearity, with linear loss and cubic gain (instead of the, respectively, linear gain and cubic loss in the cubic CGL equation), and additional quintic loss that provides for the overall stability of the model.

It is commonly known that CW states are subject to the modulational instability (MI) under the action of self-focusing nonlinearity acting in combination with anomalous group-velocity dispersion (GVD) [9,10]. Prior to fiber optics, the MI was predicted in hydrodynamics [11] and plasmas [12]. In optics, the MI was considered not only for uniform CW states, but also for extended (super Gaussian) wave packets [13]. The MI in optical fibers offers a means to generate a regular array of solitary pulses, i.e., it may serve as a source of soliton trains [14]. In this capacity, it was adapted for the use in high-bit-rate optical telecommunications [15,16].

However, when a breakup of CW and quasi-CW radiates into a train of picosecond and femtosecond pulses in the fiber, higher-order nonlinear effects such as self-steepening, self-induced Raman scattering (SRS) and higher order dispersion effects such as third-order dispersion (TOD) should also be taken into account [17]. It is well-known that TOD effects splitting-up of higher order solitons. The inelastic Raman scattering is due to the delayed response of the medium, which forces the pulse to undergo a frequency shift, which is known as self-frequency shift (SFS). The effect of self-steepening is due to the intensity-dependent group velocity of optical pulse, which gives the pulse a very narrow width in the course of propagation. Therefore, in real ultrashort optical fiber transmission systems, we must consider all these higher order effects [18]. Recently, the study of MI in higher NLS (HNLS) equation have been realized in [19]. The author demonstrated that the MI gain can exist even in the normal dispersion medium, depending on the strength of the higher-

*glatchio@yahoo.fr
†mohamali@pks.mpg.de
‡kofane@pks.mpg.de
§moubissi@hotmail.com

 

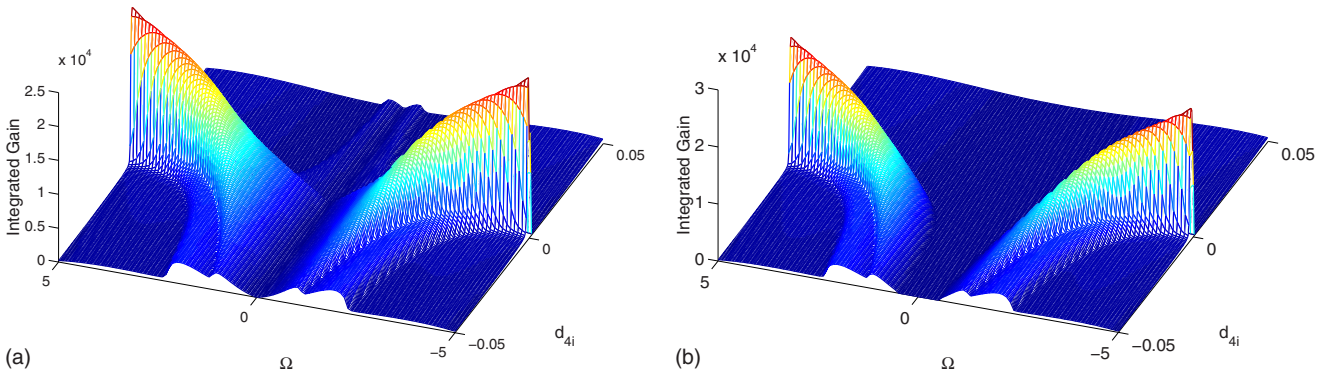


FIG. 1. (Color online) MI Integrated gain as a function of $d_{4i}$ and $\Omega$. (a) Two gain peaks appear regardless of the sign of $p_r d_{4i} < 0$ and move away from the center when $d_{4i} \to 0$, in the anomalous dispersion regime. (b) Two gain peaks appears in the normal dispersion regime when $p_r d_{4i} > 0$, while the gain disappears when $p_r d_{4i} < 0$.

order dispersion and nonlinear terms, in contrast to the NLS equation in which the MI gain occurs only in the anomalous dispersion regime [20]. The higher-order filtering terms are essential for making the model realistic, and for describing more involved pulse generation effects [21–23]. For an optical system, including bandwidth-limited gain and higher-order effects, the propagation of femtosecond pulses is governed by the generalized higher-order complex Ginzburg-Landau (GHCGL) equation with dimensionless form [21–23]

$$\begin{aligned} i\psi_z + (p_r + ip_i)\psi_{tt} + (q_r + iq_i)|\psi|^2\psi + (c_r + ic_i)|\psi|^4\psi \\ = i(\gamma_r + i\gamma_i)\psi + i(d_{3r} + id_{3i})\psi_{ttt} + i(d_{4r} + id_{4i})\psi_{tttt} \\ + i(m_r + im_i)(|\psi|^2\psi)_t + i(n_r + in_i)(|\psi|^2)_t\psi, \end{aligned} \tag{1}$$

where $\psi$ is the slowly varying envelope of complex electric field, $t$ is the retarded time and $z$ is the propagation distance. The parameters $p_r$, $p_i$, $q_r$, $q_i$, $c_r$, $c_i$, $\gamma_r$, $\gamma_i$, $d_{3r}$, $d_{3i}$, $d_{4r}$, $d_{4i}$, $m_r$, $m_i$, $n_r$, and $n_i$ are real constants. The parameter $p_r$ measures the wave dispersion, $p_i$ the spectral filtering, $q_r$ and $q_i$ represent the nonlinear coefficient and the nonlinear gain absorption coefficient, respectively. We noticed that nonlinear gain helps to suppress the growth of radiative background (linear mode), which always accompanies the propagation of nonlinear stationary pulses in real fiber links. The parameter $c_r$ and $c_i$ stand for the higher-order correction terms to the nonlinear refractive index and the nonlinear amplification absorption, respectively. The parameter $\gamma_r$ and $\gamma_i$ represent the linear gain ($\gamma_r > 0$) or loss ($\gamma_r < 0$) and the frequency shift, respectively. The complex parameter $d_3$ ($d_{3r} + id_{3i}$) is the TOD coefficient. The complex parameter $d_4$ ($d_{4r} + id_{4i}$) account for the FOD coefficient. The parameter $m_r$ is the nonlinear dispersion term (Kerr dispersion), $n_r$ and $n_i$ are the nonlinear gradient terms, which result from the time-retarded induced Raman process. In fact, $n_i$ is usually responsible for the SFS. Usually, $m_i$ and $n_r$ are neglected in the optical transmission system. When $d_3 = 0$, $d_4 = 0$, $m_r = 0$, $m_i = 0$, $n_r = 0$, and $n_i = 0$, Eq. (1) becomes the CQ CGL equation. So far, different types of solutions of the one-dimensional CGL equation such as pulselike, shocklike, sources, sinks, periodic, and quasiperiodic solutions have been analyzed [24]. Recently, the soliton solution of Eq. (1) have been investigated by many authors. Li *et al.* [21] have investigated exact solutions of Eq. (1) using a chirped hyperbolic secant type solution. Through the collective variable treatment, it has been shown that the dynamics of pulse parameters are deeply modified due to the effects of high possible values of parameters of the

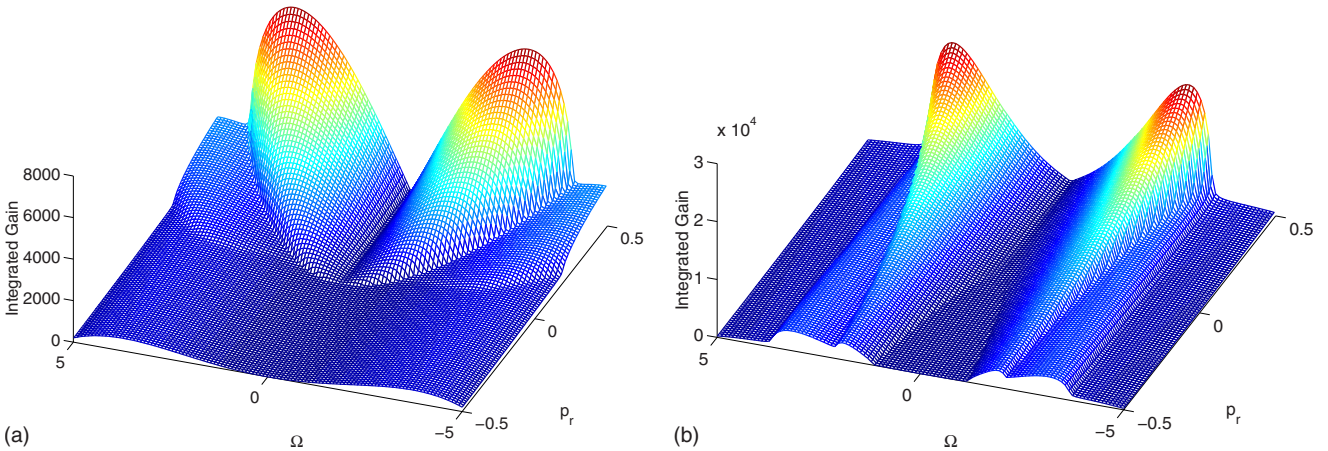


FIG. 2. (Color online) MI Integrated gain as a function of $p_r$ and $\Omega$. (a) Two gain peaks appear if $p_r d_{4i} > 0$ and disappears when $p_r d_{4i} < 0$. (b) The two gain peaks exists regardless of the sign of $p_r d_{4i}$.

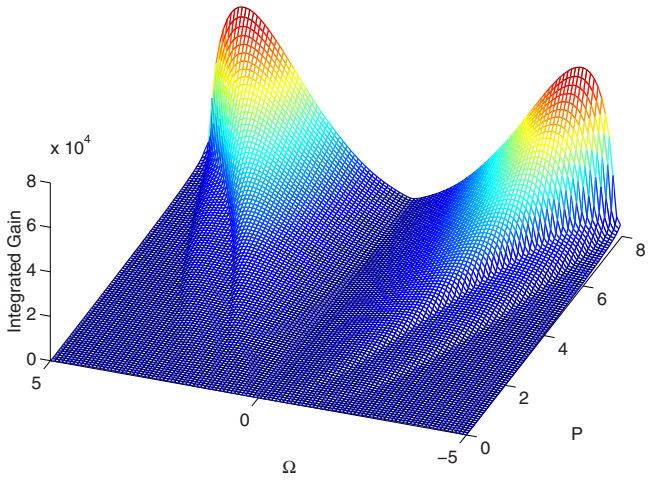


FIG. 3. (Color online) MI Integrated gain as a function of power $P$ and $\Omega$. The MI gain increases with the input power.

GHCGL equation [23]. However, MI of Eq. (1) and the dynamics of the solitons induced by the MI have not been yet performed.

In the present work, we have numerically explored the generation of structures induced by MI in the normal and anomalous dispersion regime for a large parameters space, which are not been studied in the case of the GHCGL equation. Latter, we study the long-term behavior of a periodically modulated input signal. For a typical fiber system, we choose the following physical parameter values: $1.763T_0 = 400$ fs, wavelength $\lambda = 1.55$ $\mu$m, GVD $D = \pm 0.5$ ps.nm$^{-1}$ km$^{-1}$, TOD $\beta_3 = -0.007$ ps$^3$ km$^{-1}$, nonlinear parameter $\gamma = 20$ W$^{-1}$ km$^{-1}$, the spacing of filters $Z_a = (1/M) = 0.75$, 3 dB bandwidth of the filters $\Delta\lambda = \lambda^2/(\pi c T_0 \sqrt{2(p_i)} Z_a) = 29$ nm, and nonlinear gain $g_2 = 6.8$ W$^{-1}$ km$^{-1}$. These parameters give the following dimensionless parameters: $p_i = 0.1$, $q_i = 0.5$, $c_r = 0.34$, $d_{3r} = -0.008$, $d_{3i} = 0$, $m_r = -0.025$, and $n_i = -0.05$.

The paper is organized as follows. In Sec. II, the linear stability analysis of the MI is formulated. The instability zones as well as the analytic expressions of the gain of MI are obtained. Typical outcomes of the nonlinear development of the MI, in the form of regular and irregular patterns, are reported in Sec. III. We focus on the role played by the loss/gain coefficient and higher-order dispersion terms. Section IV concludes the paper.

## II. LINEAR STABILITY ANALYSIS OF THE MODULATION INSTABILITY

Neglecting the $q_i$ and $c_i$ parameters, CW solution to Eq. (1) is given by

$$\psi(z,t) = \sqrt{P}\exp[i\phi_{NL} + (\gamma_r + i\gamma_i)z], \tag{2}$$

where $\phi_{NL} = Pq_r\int_0^z \exp(2\gamma_r z)dz + P^2 c_r \int_0^z \exp(4\gamma_r z)dz$ is the nonlinear phase shift and $P$ is the input power of the CW. To

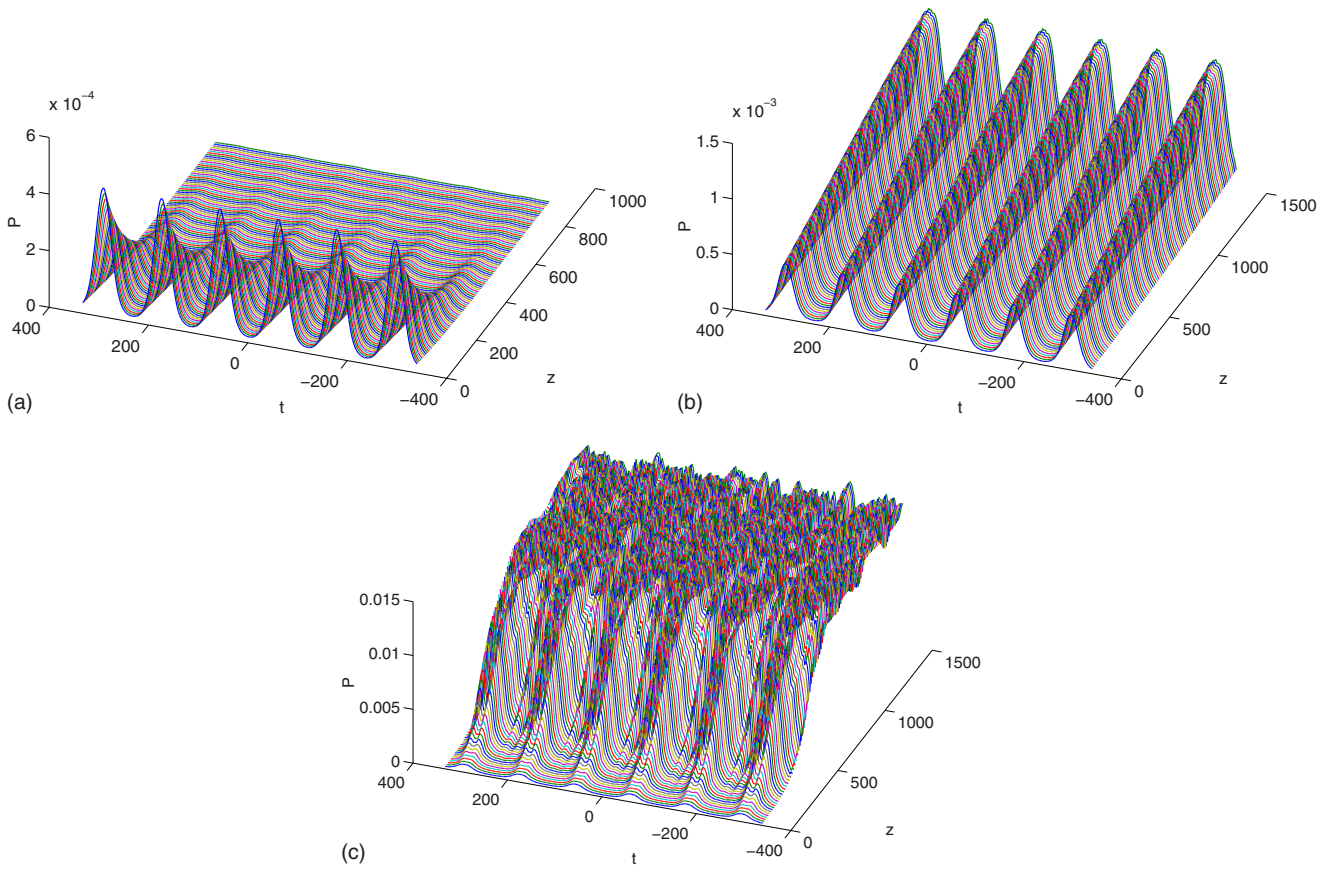


FIG. 4. (Color online) Different propagation results of the input CW in the GHCGL with anomalous dispersion. (a) Attenuation pulse for $\gamma_r = -0.003$. (b) Stable pulse for $\gamma_r = 0.0007$. (c) Chaotic pulse for $\gamma_r = 0.005$.

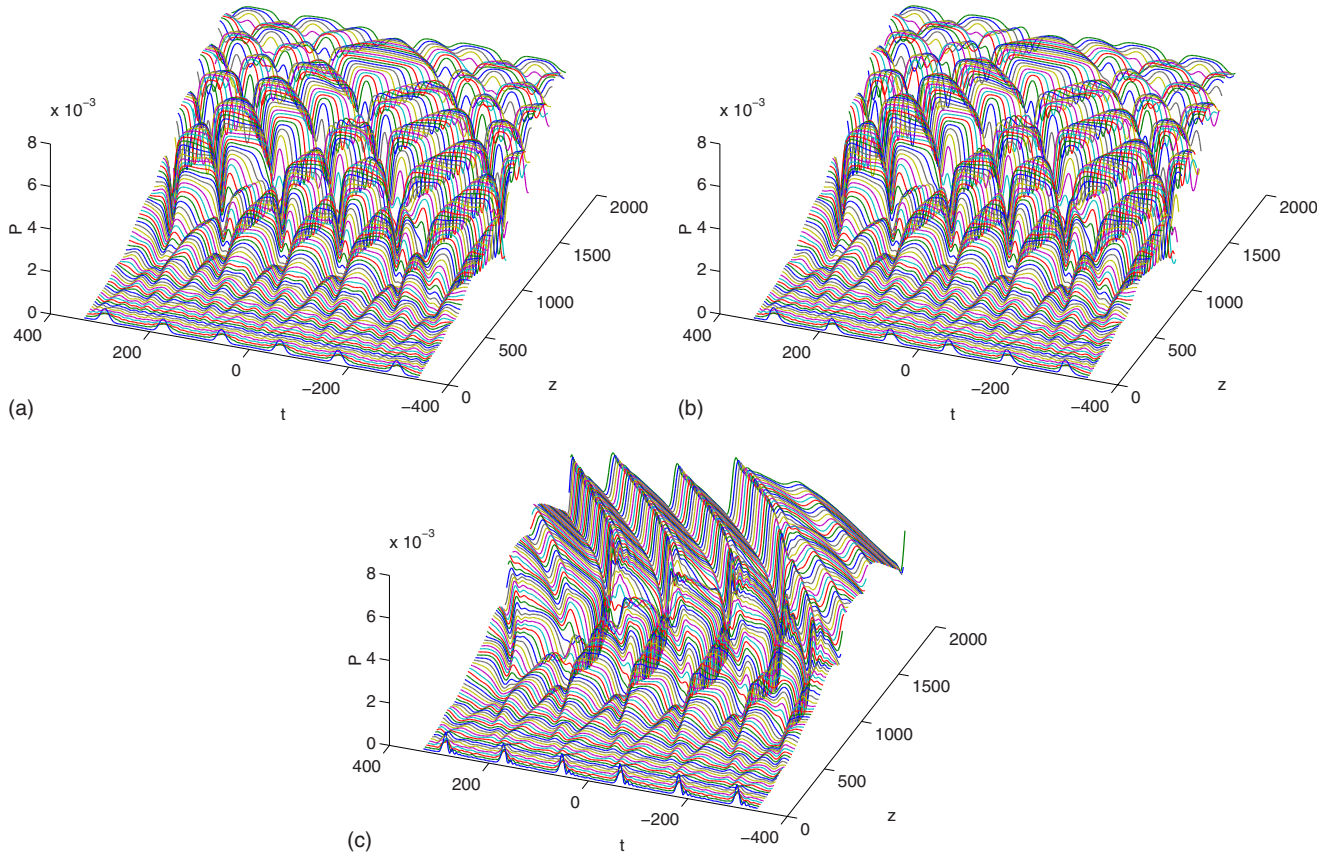


FIG. 5. (Color online) Evolution of CW showing the effects of the TOD terms $d_{3r}$ in the anomalous dispersion regime. (a) $d_{3r}=-0.008$, (b) $d_{3r}=-0.08$, (c) $d_{3r}=-0.8$.

analyzed the MI of CW solution Eq. (2), we introduce the perturbed electric field

$$\psi(z,t) = (\sqrt{P} + u + iv)\exp[i\phi_{NL} + (\gamma_r + i\gamma_i)z] \tag{3}$$

and linearizing Eq. (1) in $u$ and $v$, we obtain the following set of two coupled equations:

$$\begin{aligned} u_z =& -p_r v_{tt} - p_i u_{tt} + d_{3r} u_{ttt} - d_{3i} v_{ttt} + d_{4r} u_{tttt} - d_{4i} v_{tttt} \\ &+ (3m_r + 2n_r)Pf(z)u_t - m_i Pf(z)v_t \end{aligned}$$

$$\begin{aligned} v_z =& p_r u_{tt} - p_i v_{tt} + d_{3r} v_{ttt} + d_{3i} u_{ttt} + d_{4r} v_{tttt} + d_{4i} u_{tttt} \\ &+ 2Pf(z)[q_r + 2c_r Pf(z)]u + (3m_i + 2n_i)Pf(z)u_t \\ &+ m_r Pf(z)v_t, \end{aligned} \tag{4}$$

where $f(z)=\exp(2\gamma_r z)$. These equations can be solved approximately by assuming a solution of the form [25]

$$u(z,t) = u_0(z)\exp\left[i\int K(z)dz - i\Omega t\right]$$

$$v(z,t) = v_0(z)\exp\left[i\int K(z)dz - i\Omega t\right], \tag{5}$$

where $K$ and $\Omega$ represent, respectively, the wave number and the frequency of the modulation. By substituting Eq. (5) into Eq. (4), and assuming that $u_0$ and $v_0$ vary slowly with $z$ ($\frac{\partial u_0}{\partial z} = \frac{\partial v_0}{\partial z} \cong 0$), the wave number $K$ is found to satisfy the following dispersion relation

$$(K + g_r + ig_i)^2 = \Delta_r + i\Delta_i, \tag{6}$$

where

$$\begin{aligned} g = (g_r + ig_i) =& [P\Omega f(z)(2m_r + n_r) - \Omega^3 d_{3r}] \\ &+ i[\Omega^2(p_i + \Omega^2 d_{4r})] \end{aligned}$$

$\Delta_r$ and $\Delta_i$ are given in the appendix. Therefore,

$$K(\Omega,z) = -g_r \pm h_1 + i(-g_i \pm h_2), \tag{7}$$

where

$$h_1 = \frac{1}{2}\sqrt{\frac{\Delta_r + |\Delta|}{2}}, \quad h_2 = \frac{1}{2}\sqrt{\frac{-\Delta_r + |\Delta|}{2}}.$$

In the absence of the loss/gain coefficient ($\gamma_r=0$), $K$ becomes $z$ independent. MI occurs whenever $K$ has a negative imaginary part since the perturbation then grows exponentially along the fiber length. The asymptotic behavior of the extended nonlinear plane wave is then determined by the sign of the quantity $-g_i-h_2$. Since the coefficient $h_2$ is always positive, the inequality $-g_i-h_2<-g_i+h_2$ holds. The difference $-g_i-h_2$ is always negative if $g_i>0$, and then the perturbation grows up when the propagation distance $z$ tends to infinity, i.e., the system remains unstable under modulation. On the other hand, if $g_i<0$, the asymptotic behavior of the

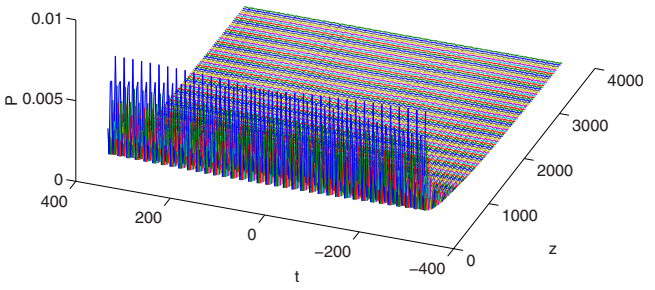


FIG. 6. (Color online) Evolution of the input CW out of the MI zones in the anomalous dispersion regime. The train of solitons disappears and form a constant background solution.

system will depend on the sign of $-g_i-h_2$. In what follows we study the cases where MI appear.

(1) First of all, if $-g_i-h_2<0$, we see that the imaginary part of $K$ is negative, and the system is said to be modulationally unstable. This inequality allows us to write the MI criterion for the CW in the GHCGL as

$$\Delta_i^2 - 4(g_i + \Delta_r)g_i > 0. \tag{8}$$

The domain of MI is determined by the inequality $g_i<0$. Then we have

$$d_{4r}\Omega^4 + p_i\Omega^2 < 0. \tag{9}$$

The boundaries of the MI domain are then given by

$$-\Omega_0 \le \Omega \le \Omega_0, \tag{10}$$

where

$$\Omega_0 = (-p_i/d_{4r})^{1/2},$$

which satisfies the constraint $-p_i/d_{4r}<0$. The MI gain defined as $g(\Omega)=2|\mathrm{Im}(K)|$ [9] as

$$g(\Omega) = 2(g_i + h_2). \tag{11}$$

We note that the real part of the TOD ($d_{3r}$) does not contribute to the MI gain.

(2) Second, from the above calculations, we can deduce that, when the imaginary part of $K$ is positive $-g_i-h_2>0$, we obtain the following criterion

$$\Delta_i^2 - 4(g_i + \Delta_r)g_i < 0. \tag{12}$$

This result means that CW, which verify Eq. (12) are stable under modulation.

However in the presence of the loss/gain coefficient, the wave number $K$ depend on the propagation distance. The MI gain spectrum of the fiber at the distance $L$ can be calculated as a function of the MI frequency by the relation $g(\Omega)=2\int_0^L|\mathrm{Im}[K(\Omega,z)]|dz$ [25]. Since the expression of $g_i$ is not function of the loss/gain coefficient, we conclude that the MI

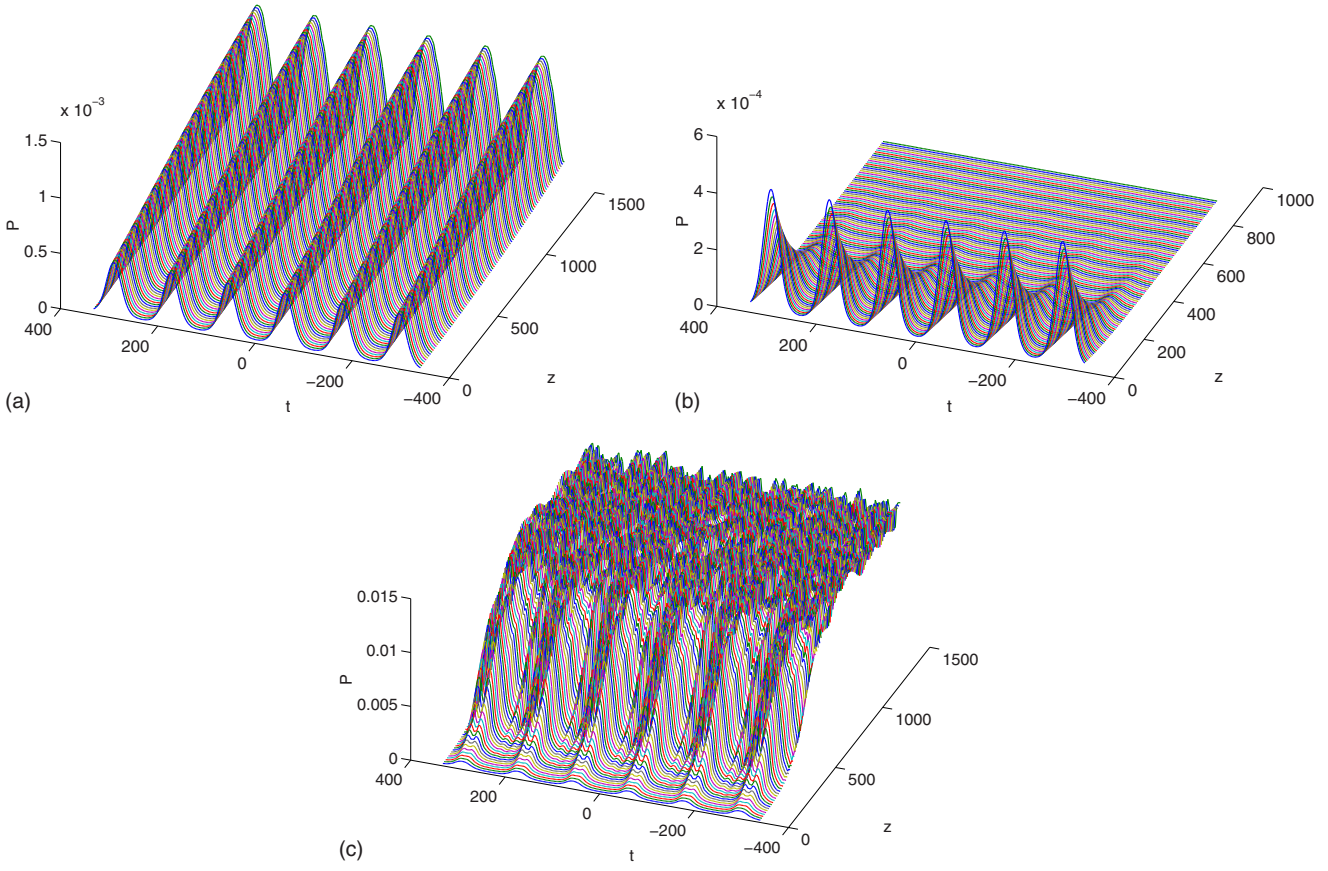


FIG. 7. (Color online) Evolution of the input CW in the normal dispersion regime. (a) Stable pulse for $\gamma_r=0.0007$, (b) Attenuation pulse for $\gamma_r=-0.004$, (c) Chaotic pulse for $\gamma_r=0.005$.

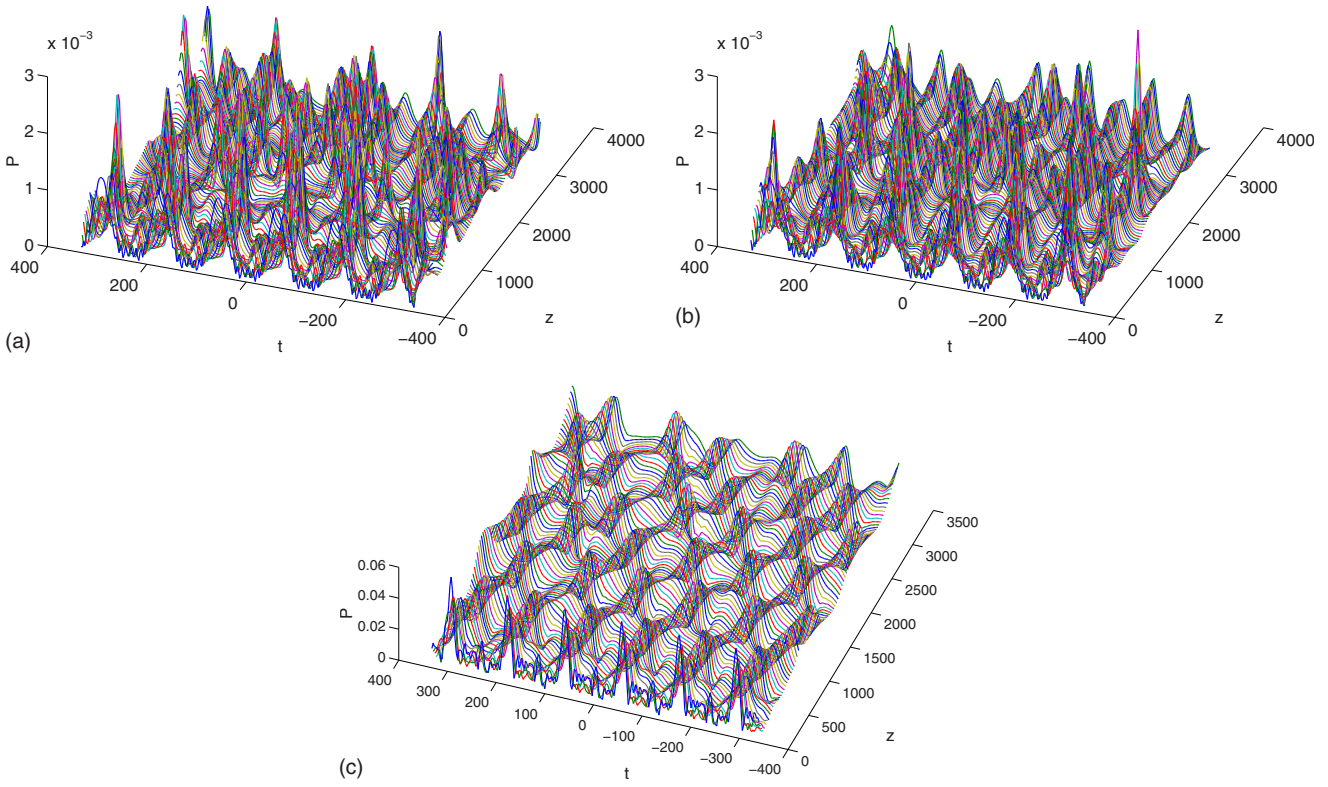


FIG. 8. (Color online) Evolution of CW showing the effects of the TOD terms $d_{3r}$ in the normal dispersion regime. (a) $d_{3r}=-0.008$, (b) $d_{3r}=-0.08$, (c) $d_{3r}=-0.8$.

boundaries are also given by relation (10). By choosing $d_{4r}=-0.0001$, and $p_i=0.1$, we obtain $\Omega_0=31.62$. We calculate the MI gain at the distance $L=1500$ m numerically by chosen the frequency inside the above MI zones. Figure 1 portrays the MI gain as a function of the FOD coefficient $d_{4i}$ and the frequency $\Omega$, with fixed values for $p_r$ and $P$. Figure 1(a) shows the spectra for the case of the anomalous dispersion regime $p_r=0.5$. Two gain peaks are shown here and interestingly is the fact that another gain peaks appears and move away from the center when $d_{4i}\to 0$. Figure 1(b) plot the gain spectra for the case of the normal dispersion regime $p_r=-0.5$. We find that two gain peaks appears when $p_r d_{4i}>0$ and disappears when $p_r d_{4i}<0$, while nonzero gain exists regardless of the signs of $p_r$ and $d_{4i}$ as shown in Fig. 1(a).

Figure 2 displays the MI gain spectrum as functions of $p_r$ and $\Omega$ with fixed values for $d_{4i}$ and $P$. We find in Fig. 2(a) that two gain peaks appears if $p_r d_{4i}>0$ and disappears when $p_r d_{4i}<0$. We find also the presence of the two gain peaks in Fig. 2(b), but in comparison with Fig. 2(a), the nonzero gain exists regardless of the sign of the product $p_r d_{4i}$. Then we can conclude that the gain spectrum is sensitive to the sign of the FOD coefficient. It is also interesting to monitor the evolution of the MI spectrum with variation of total power $P$ and modulational frequency $\Omega$. These results are displayed in Fig. 3 and we can see that the MI gain increases with the input power.

## III. NUMERICAL SIMULATION OF THE MODULATIONAL INSTABILITY

The next step of the analysis is to run direct simulation of Eq. (1), adding small initial modulational perturbations to CW states, with the objective to identify nonlinear patterns generated by the MI. The MI is induced by injecting an input signal in the form [9]

$$\psi(0,t)=\sqrt{P}[1+a_m\sin(\Omega_m t)]\exp(i\phi_{NL}), \tag{13}$$

where $a_m=0.09$ is the modulation amplitude and $\Omega_m=0.75$ is the frequency of a weak sinusoidal modulation imposed on the CW beam, which belong to the above MI zones [see relation Eq. (10)]. Equation (1) with initial condition Eq. (13) is solved utilizing the split-step fourier method [9]. During simulations, we focus on the role played by the loss/gain coefficient and higher-order dispersion terms.

### A. Ultrashort solitonlike pulses in the anomalous dispersion regime

Results of numerical simulations on the MI in the anomalous dispersion regime as a function of the loss/gain coefficient are presented in Fig. 4. Obviously, depending on the value of the loss/gain coefficient, one observes different kind of propagation. For $\gamma_r=-0.003$, the propagation of waves presents an attenuation of pulses as shown in Fig. 4(a): the amplitude of wave decreases gradually during the propagation. For $\gamma_r=0.0007$, the propagation of waves remains stable as shown in Fig. 4(b). Waves keep their shape and their amplitude remains constant during the propagation. The pulse can propagate stably in the given distance, even in the presence of the higher-order dispersion and nonlinear terms. In fact, it is well known that the TOD caused an asymmetrical broadening in the time domain, the self-steepening

caused a spectral broadening of the pulse and the SFS is responsible of the time-retarded induced Raman process. However, there exists a balance of the cooperation of all these effects, which lead to a stable pulse propagation. But, for $\gamma_r=0.005$, the MI development leads to an irregular pattern, with a quasichaotic field configuration as shown in Fig. 4(c). In Fig. 5, we investigate effects of the coefficient $d_{3r}$ on the dynamical behavior of the system. Figure 5(a) shows the propagation of the initial CW through the system for $d_{3r}=-0.008$, while Fig. 5(b) stands for $d_{3r}=-0.08$, and lastly Fig. 5(c) is depicted for $d_{3r}=-0.8$. Even though the coefficient $d_{3r}$ does not directly influence the MI gain spectrum, one sees that as this term decreases, its has an effect on the direction of soliton which propagate [see Fig. 5(c)]. However, the FOD term does not alter the dynamics of the soliton.

Now we choose the modulational frequency as $\Omega_m=40$, which is outside the MI boundaries defined above. We observe in Fig. 6 that the train of solitons produce initially tend to disappear as the soliton evolves in propagation distance $z$. The system is then said to be stable under modulation.

### B. Ultrashort solitonlike pulses in the normal dispersion regime

Results of numerical simulations on the MI in the normal dispersion regime as a function of the loss/gain coefficient are presented in Fig. 7. The evolution of the initial CW up to a distance $z=1500$ m is shown in Fig. 7(a) for $\gamma_r=0.0007$, where it was found that the pulse can propagate stably in the normal dispersion regime. For $\gamma_r=-0.004$, we observe in Fig. 7(b) that the input CW decays into a zero solution during the propagation. In the case presented in Fig. 7(c), We observe that the trains of solitons which are initially stable falls into chaotic regime for $\gamma_r=0.005$. We observe in Fig. 8 that while one decreases the coefficient $d_{3r}$, the direction of propagation of soliton is modified such as in Fig. 5. Here, one views that the generation of pulses train seem to be chaotic. The FOD does not alter the dynamics of the soliton. Also in the case of normal dispersion regime, when the modulational frequency is chosen as $\Omega_m=40$, which is outside the MI boundaries, the train of solitons disappear progressively as the propagation distance $z$ increases as shown in Fig. 9, which leads the system to a stable regime.

## IV. CONCLUSION

In this work, we have investigated the MI of the CW in the generalized GHCGL with the TOD and FOD, and the cubic-quintic nonlinear terms. This equation describes the propagation of an ultrashort femtosecond optical pulses. The instability regions have been determined by using the linear stability analysis. Analytic expression of the MI gain have been derived. We have found that the gain is independent to the real part of the TOD coefficient, but is sensitive to the sign of the FOD coefficient. Numerical simulations have been performed to investigate the outcome of nonlinear development of the MI of the underlying GHCGL. We have found that when the modulational frequency belong to the

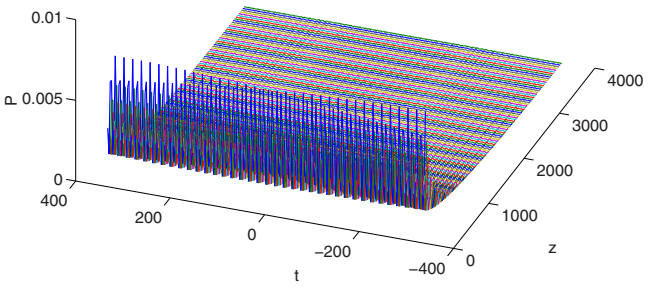


FIG. 9. (Color online) Evolution of the input CW out of the MI zones in the normal dispersion regime. The train of solitons disappears and form a constant background solution.

MI zones, the initial CW tends to be disintegrated into a train of solitonlike objects. Attenuation waves as well as chaotic pulses are also observed during the propagation. However, when the modulational frequency is out of the MI zones, the trains of solitons disappear progressively and form a constant background solution. We have also found that even though the real part of the TOD does not contribute to the MI gain, it influences the evolution of MI and the dynamics of the pulse train generated. Excellent agreement has been obtained between our theoretical and numerical approaches. The present result, especially the formation of the stable periodic array of localized pulses, may find straightforward application in nonlinear optics.

## ACKNOWLEDGMENTS

A.M. and T.C.K. are grateful for the hospitality of the Max-Planck Institute for the Physics of Complex Systems in Dresden.

## APPENDIX

Elements of the dispersion relation defined by Eq. (6) are:

$$\Delta_r = L_8\Omega^8 + L_6\Omega^6 + L_4\Omega^4 + L_2\Omega^2 + L_0,$$

$$\Delta_i = L_7\Omega^7 + L_5\Omega^5 + L_3\Omega^3 + L_1\Omega,$$

$$L_8 = d_{4i}^2, \quad L_7 = 2d_{3i}d_{4i}, \quad L_6 = -d_{3i}^2 - 2p_r d_{4i},$$

$$L_5 = -2Pf(z)(2m_i n_i)d_{4i} - 2p_r d_{3i},$$

$$L_4 = 4Pf(z)m_i n_i d_{3i} + p_r^2 + 2Pf(z)[q_r + 2c_r Pf(z)]d_{4i},$$

$$L_3 = 4Pf(z)m_i n_i p_r + 2Pf(z)[q_r + 2c_r Pf(z)]d_{3i},$$

$$L_2 = (m_r - n_r)^2 P^2 f(z)^2 - 3P^2 f(z)^2 m_i^2 - 2P^2 f(z)^2 m_i n_i - 2Pf(z)[q_r + 2c_r Pf(z)]p_r,$$

$$L_1 = -2P^2 f(z)^2 (m_r + n_r)q_i - 4P^3 f(z)^3 (m_r + n_r)c_i - 2P^2 f(z)^2 [q_r + 2c_r Pf(z)]m_i,$$

$$L_0 = P^2 f(z)^2 [q_r + 2c_r Pf(z)]^2.$$

[1] Yu. S. Kivshar and G. P. Agrawal, *Optical Solitons: From Fibers to Photonic Crystals* (Academic, San Diego, 2003).
[2] A. Hasegawa and F. Tappert, Appl. Phys. Lett. **23**, 142 (1973); **23**, 171 (1973).
[3] L. F. Mollenauer, R. H. Stolen, and J. P. Gordon, Phys. Rev. Lett. **45**, 1095 (1980).
[4] V. E. Zakharov and A. B. Shabat, Sov. Phys. JETP **34**, 62 (1972).
[5] J. N. Kutz, C. V. Hile, W. L. Kath, R.-D. Li, and P. Kumar, J. Opt. Soc. Am. B **11**, 2112 (1994); B. Sandstede, C. K. R. T. Jones, and J. C. Alexander, Physica D **106**, 167 (1997).
[6] A. Hasegawa and Y. Kodama, *Solitons in Optical Communication* (Oxford University Press, New York, 1995).
[7] B. A. Malomed, M. Goelles, I. M. Uzunov, and F. Lederer, Phys. Scr. **55**, 73 (1997); M. Nakazawa, H. Kubota, K. Suzuki, E. Yamada, and A. Sahara, Chaos **10**, 486 (2000).
[8] L. M. Hocking and K. Stewartson, Proc. R. Soc. London, Ser. A **326**, 289 (1972); N. R. Pereira and L. Stenflo, Phys. Fluids **20**, 1733 (1977).
[9] G. P. Agrawal, *Nonlinear Fiber Optics* (Academic, San Diego, 2001).
[10] G. L. Alfimov, A. R. Its, and N. E. Kulagin, Theor. Math. Phys. **84**, 787 (1990); F. Kh. Abdullaev, S. A. Darmanyan, and J. Garnier, Prog. Opt. **44**, 303 (2002).
[11] L. A. Ostrovskii, Sov. Phys. JETP **24**, 797 (1967); T. B. Benjamin and J. E. Feir, J. Fluid Mech. **27**, 417 (1967).
[12] V. I. Karpman, JETP Lett. **6**, 277 (1967).
[13] M. Nakazawa, K. Suzuki, H. Kubota, and H. A. Haus, Phys. Rev. A **39**, 5768 (1989).
[14] A. Hasegawa and W. F. Brinkman, IEEE J. Quantum Electron. **16**, 694 (1980).
[15] G. Millot, P. Tchofo Dinda, E. Seve, and S. Wabnitz, Opt. Fiber Technol. **7**, 170 (2001).
[16] G. Millot, S. Pitois, J. M. Dudley, and M. Haelterman, in *Optical Solitons—Theoretical and Experimental Challenges*, edited by K. Porsezian and V. C. Kuriakose (Springer-Verlag, Berlin, 2003).
[17] R. Ganapathy and V. C. Kuriakose, Pramana, J. Phys. **58**, 669 (2002); R. Ganapathy, K. Senthilnathan, and K. Porsezian, J. Opt B: Quantum Semiclassical Opt. **6**, S436 (2004).
[18] Z. Li, L. Li, H. Tian, and G. Zhou, Phys. Rev. Lett. **84**, 4096 (2000).
[19] W. P. Hong, Z. Naturforsch. **61**, 225 (2006); W. P. Hong, Opt. Commun. **213**, 173 (2002).
[20] P. D. Drummond, T. A. B. Kennedy, J. M. Dudley, R. Leonhardt, and J. D. Harvey, Opt. Commun. **78**, 137 (1990).
[21] J. Tian, H. Tian, and G. Zhou, Phys. Scr. **71**, 507 (2005); Z. Li, L. Li, H. Tian, G. Zhou, and K. Spatschek, Phys. Rev. Lett. **89**, 263901 (2002).
[22] A. Mohamadou, B. E. Ayissi, and T. C. Kofane, Phys. Rev. E **74**, 046604 (2006); F. II. Ndzana, A. Mohamadou, and T. C. Kofane, Opt. Commun. **275**, 421 (2007).
[23] S. I. Fewo, C. M. Ngabireng, and T. C. Kofane, J. Phys. Soc. Jpn. **77**, 074401 (2008).
[24] W. van Saarloos and P. C. Hohenberg, Physica D **56**, 303 (1992).
[25] G. P. Agrawal, IEEE Photon. Technol. Lett. **4**, 562 (1992).